

Carrier-envelope-phase effect in nonsequential double ionization of Ar atoms by few-cycle laser pulses

Fengzhen Feng (冯凤珍) and Lihua Bai (白丽华)*

College of Science, Shanghai University, Shanghai 200444, China

*Corresponding author: binger@shu.edu.cn

Received January 25, 2018; accepted April 16, 2018; posted online May 28, 2018

A classical ensemble method is used to investigate nonsequential double ionization (NSDI) of Ar atoms irradiated by linearly polarized few-cycle laser pulses. The correlated-electron momentum distribution (CMD) exhibits a strong dependence on the carrier-envelope phase (CEP). When the pulse duration is four cycles, the CMD shows a cross-like structure, which is consistent with experimental results. The CEP dependence is more notable when the laser pulse duration is decreased to two cycles and a special L-shaped structure appears in CMD. Recollision time of returning electrons greatly depends on CEP, which plays a significant role in accounting for the appearance of this structure.

OCIS codes: 320.7120, 190.7110, 270.6620.

doi: 10.3788/COL201816.063201.

The phenomena induced by interaction of atoms with intense laser pulses are always hot topics in atomic and molecular physics^[1,2]. Double ionization (DI), for one, has attracted considerable attention. In the process of exploring atomic DI in a strong laser field, electron-electron correlation^[3,4] (EEC) plays a significant role and dramatically changes previous physical images based on single-active-electron (SAE) approximation^[5]. EEC has been found in the process of nonsequential DI (NSDI), which has drawn much attraction in recent years^[6-9]. NSDI indicates an unusual EEC process, where the next ionization of the outermost electrons of an atom is closely related to the previous ionized electron. Extensive experiments and theoretical researches have provided strong evidence that the rescattering mechanism^[10] is responsible for the NSDI process. According to this mechanism, one electron is released by tunneling ionization and, then, is driven back near its parent core to knock out the bound electron when the laser field changes its direction. There are two different ionization mechanisms^[10] in NSDI based on the rescattering mechanism. The bound electron can be ionized directly if the energy of the returning electron is larger than that of the ionization potential of the bound electron; this direct ionization channel is defined as recollision-impact ionization (RII). If the energy of the returning electron is not large enough to directly knock out the bound electron, then the NSDI process is still possible via the recollision excitation with subsequent ionization (RESI). In this case, the bound electron is excited by recollision (RC) and is ionized at the subsequent extremum of the laser pulse.

With the rapid development of laser technology, an ultrafast laser with pulses as short as a few optical cycles has been available^[11-13]. Researches about NSDI on the time scale of a few optical cycles have attracted great attention^[14,15]. Few-cycle laser pulses can ensure only one RC contributing to NSDI and avoid multiple collisions. Furthermore, in such few-cycle laser pulses, NSDI of atoms

varies greatly with the carrier-envelope phase^[16,17] (CEP), which means the phase of the carrier frequency with respect to the envelope. In turn, the behavior of correlated electrons in NSDI can be manipulated by regulating the CEP. It has been discovered that momentum distribution along the laser polarization axis has a pronounced CEP dependence for Ar²⁺ in 4 fs laser pulses^[18]. Recently, Bergues *et al.* have confined the DI of Ar atoms to a single laser cycle by using near-single-cycle laser pulses with averaged CEP and have obtained a cross-like structure^[19] in correlated-electron momentum distribution (CMD). CMD is a crucial tool to reveal the EEC effect in NSDI. Many novel phenomena, such as the V-like shape^[20], the cross-like structure^[19,21], and the transition from anticorrelation to correlation^[22] have been observed in CMD. In recent years, the studies of NSDI in a two-color field caught more and more researchers' attention. Zhou *et al.* find the arc shape in the CMDs in the two-color field^[15]. The anticorrelation behavior of electrons is also found in the two-color field^[23].

In this Letter, by using a classical ensemble method, we first investigate the NSDI of Ar atoms irradiated by linearly polarized four-cycle laser pulses with different CEPs. For four-cycle laser pulses, the CMD shows a cross-like structure with an averaged CEP, which is coincident with the result in the experiment^[19]. Furthermore, the NSDI of Ar atoms strongly depends on the CEP; the CMDs present an apparent shift from the third quadrant to the first quadrant with the increasing CEP. We observe the electron trajectories at different times and find that the competition of the RC time corresponds with the transition of electron pairs in CMDs. Subsequently, the NSDI in two-cycle laser pulses is investigated. A special L-shaped structure is found in the CMD. The appearance of the L-shaped structure is correlated to the RC time of returning electrons. RC events occurring around the zero crossing of the laser field will cause the side-by-side

electrons (emission electrons with the same direction), while the RC events clustering near the peaks of the laser field eventually cause the back-to-back electrons (emission electrons with the opposite direction). Back analysis manifests that asymmetric energy allocation at different RC times causes the different emission directions of two electrons.

The method we use is the classical ensemble method based on the numerical solutions to the time-dependent Newton equation (TDNE). The classical ensemble method has been widely used to describe the strong-field DI process^[24,25] and achieves great success in studying the NSDI phenomena. The best advantage of this method is trajectory-back analysis, which means that people can back-analyze the trajectories they are interested in.

The light-free Hamiltonian of a two-active-electron atom can be written as (in atomic units, a.u.)

$$H_e = \sum_{i=1}^2 \left(\frac{\mathbf{p}_i^2}{2} - \frac{2}{\sqrt{\mathbf{r}_i^2 + a^2}} \right) + \frac{1}{\sqrt{\mathbf{r}_{12}^2 + b^2}}, \quad (1)$$

where \mathbf{r}_i and \mathbf{p}_i denote the position and momentum for the i th electron, respectively. The soft-core potential a is set to 1.5, and b is set to 0.05 for Ar atoms to avoid autoionization. To obtain the initial value, the ensemble is populated within the classically allowed region for Ar ground-state energy of -1.59 a.u. For each member, the positions of two electrons are assigned randomly within the allowed region by a Gaussian random series. The total kinetic energy (the ground-state energy minus the total potential energy) is assigned randomly to two electrons. The electrons are allowed to evolve in sufficient time to get a stable initial ensemble in the absence of the external laser field. Subsequently, we turn on the external laser field. The Hamiltonian of a two-active-electron atom in a laser pulse is given by

$$H = H_e + (\mathbf{r}_1 + \mathbf{r}_2) \cdot \mathbf{E}(t), \quad (2)$$

where the electric field of the laser pulse is written as $\mathbf{E}(t) = E_0 f(t) \cos(\omega t + \varphi) \hat{\mathbf{x}}$, E_0 , ω , and φ denote the amplitude, frequency, and CEP of the laser field, respectively, and $\hat{\mathbf{x}}$ is a unit vector along the laser polarization direction. $f(t) = \sin^2(\pi t/NT)$ is the pulse envelope, and T is the field oscillating period. N is the number of the laser cycles in the pulse. The motions of two electrons in the laser field are determined by the TDNE with

$$\frac{d\mathbf{r}_i}{dt} = \frac{\partial H}{\partial \mathbf{p}_i}, \quad \frac{d\mathbf{p}_i}{dt} = -\frac{\partial H}{\partial \mathbf{r}_i}. \quad (3)$$

The above TDNE is solved by using the standard from fourth to fifth and Runge to Kutta algorithm. At the end of the laser pulse, we record the DI events, which are defined if both electrons achieve positive energies^[22]. We record the RC time and DI time of every NSDI event. Two ionization mechanisms are distinguished by the time

interval between RC and DI, where the time interval is less than $0.1T$ for RII and larger than $0.3T$ for RESI^[26].

We first calculate the NSDI of Ar atoms irradiated by four-cycle laser pulses of a 750 nm central wavelength. In calculation, the laser intensity is chosen as 3×10^{14} W/cm². Figure 1 shows the CMDs in the major polarization axis (x axis) of the laser field with different CEPs; the horizontal axis and the vertical axis represent the momentum component of the two electrons along the x direction. Figure 1(a) exhibits the CMD with averaged CEP, in which a cross-like structure appears; this structure is similar in shape to the experimental and theoretical results^[19,21]. The bright regions appear principally in the first and the third quadrants, indicating most electrons tend to emit into the same direction. Figures 1(b)–1(d) exhibit the CMDs with CEP $\varphi = -\pi/3$, $\pi/4$, and $5\pi/6$, respectively. With the increase of CEP, the CMDs display distinct variation. When the CEP is $\varphi = -\pi/3$ [Fig. 1(b)], the bright regions appear mainly in the third quadrant and distribute around the coordinate axis, which indicates that the values of the final momentum of these two electrons are different. Figure 1(c) depicts the CMD for CEP of $\varphi = \pi/4$, the bright regions begin to transform to the first quadrant, and the structure in the third quadrant is brighter than that in the first quadrant, indicating most electrons still emit along the $-x$ direction. When the CEP is $\varphi = 5\pi/6$ [Fig. 1(d)], the bright regions in the first quadrant become clearer, and the structure in the third quadrant becomes dim. This indicates that most electrons emit into the x direction. In intense laser pulses, the NSDI of Ar atoms is dominated by the RII mechanism. In this mechanism, two electrons obtain almost the same drift momentum after RC and tend to emit into the same direction^[22]. In our calculation, the electrons of the RII mechanism occupy nearly 60% of NSDI events according to statistical data, so most electrons emit in a side-by-side manner.

In order to explore the bright regions in the first and third quadrants of Fig. 1, we count the number of RC events as a function of time in Fig. 2, where the counts have been normalized for ease of analysis. The RC time

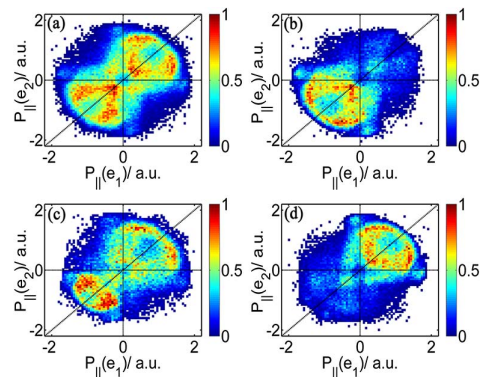


Fig. 1. CMDs of NSDI for Ar atoms in linearly polarized four-cycle laser pulses with laser wavelength of 750 nm and laser intensity of 3×10^{14} W/cm². The CEP φ is (a) all CEPs averaged, (b) $-\pi/3$, (c) $\pi/4$, and (d) $5\pi/6$, respectively.

is defined to be the instant when the distance between the returning electron and the parent core is the closest^[22]. The corresponding CEPs in Figs. 2(a)–2(c) are the same as those in Figs. 1(b)–1(d). In Fig. 2(a), as CEP $\varphi = -\pi/3$, two groups of the RC events are found, and these two groups correspond to the time at t_1 and t_2 , respectively. These two groups correspond to the primary structures of CMDs in Fig. 1. The electrons in the third quadrant are mainly due to RC events located at t_1 , whereas the electrons in the first quadrant are mainly due to RC events located at t_2 . The population located at t_1 is larger than that at t_2 , and therefore, the electron pairs in Fig. 1(b) principally distribute in the third quadrant. As the CEP increases to $\varphi = \pi/4$, as shown in Fig. 2(b), the group located at t_1 is subdued, but the population located at t_2 is enhanced. At this point, in Fig. 1(c), the electron pairs in the first quadrant increase. In Fig. 2(c), as the CEP $\varphi = 5\pi/6$, the population located at t_2 is dominant, but the population located at t_1 is suppressed, corresponding to the situation in Fig. 1(d), where most electron pairs populate in the first quadrant. Some RC events occur at an adjacent half-cycle labeled t_3 . It is found that the competition of RC times corresponds to the change of the CMDs in Figs. 1(b)–1(d). The electrons in adjacent groups emit into opposite directions. CEP influences the RC time of returning electrons, and thus influences the CMDs in Fig. 1.

In the above calculation, the NSDI of Ar atoms exhibits a distinct CEP effect. Does this effect still exist in shorter laser pulses? The NSDI of Ar atoms by shorter-cycle laser pulses is worthy of research. We decrease the pulse

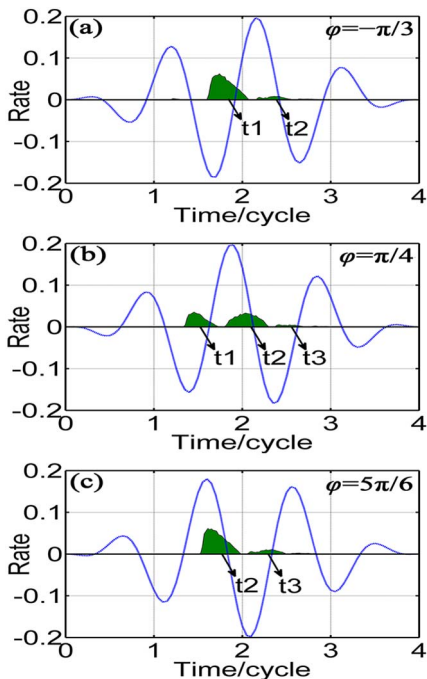


Fig. 2. Recollision trajectories counts versus time for different CEPs from Figs. 1(b)–1(d). The blue curves represent the laser field along the x axis.

duration to two optical cycles, but keep the laser intensity and laser wavelength unchanged, and then investigate the variation of the CMDs with different CEPs. Figure 3 shows the CMDs along the x axis of two-cycle laser pulses with different CEPs. When the CEP is $\varphi = 0$, as shown in Fig. 3(a), bright regions mainly locate in the second and fourth quadrants, and the majority of electrons emit in the back-to-back manner. This implies an apparent anti-correlated behavior. When the CEP $\varphi = \pi/4$, as shown in Fig. 3(b), the electron pairs locate in the first quadrant, which means that more and more electrons emit into the same direction.

What is more interesting is the appearance of the L-shaped region in the third quadrant when the CEP increases to $\pi/2$ [Fig. 3(c)]. The L-shaped structure mainly consists of electron pairs in the second, third, and fourth quadrants. In Fig. 3(d), the L-shaped structure becomes obscure and expands a bright arch-shaped structure when the CEP increases to $5\pi/6$.

In order to investigate the appearance of the L-shaped structure, we count the number of single ionization (SI) events and RC events as a function of time, respectively. In our calculation for two-cycle laser pulses, the percentage of RII electrons is almost 83%. Because there is a very short interval between RC and DI, the RC events versus time distribution are similar to the DI events versus time distribution. We only focus on the SI and RC events' distribution. The counts have been given normalized treatment. The SI time is defined to be the first time when one of the two electrons obtains positive energy. Figure 4 displays the counts of SI and RC events versus time for CEP $\varphi = 0, \pi/4, \pi/2$, and $5\pi/6$, respectively. The important peaks and zeros of the laser field are labeled H1, H2, H3, and Z1, Z2, respectively. When the CEP is $\varphi = 0$, as shown in Fig. 4(a), the SI events mainly occur near the first two peaks (H1, H2) of the laser field. The first electron is released via tunneling ionization at the time t_1 or t_2 . When the CEP is $\varphi = \pi/4$ [Fig. 4(b)], compared with Fig. 4(a), there is a great decrease of the amount of SI electrons near the time t_1 , which is coincident with the result

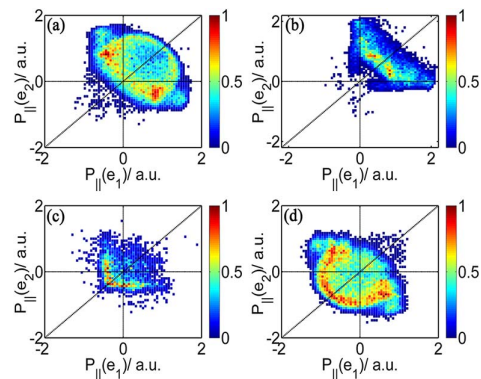


Fig. 3. CMDs in NSDI of Ar atoms by 750 nm linearly polarized two-cycle laser pulses with laser intensity at 3×10^{14} W/cm². The CEP φ is chosen as (a) 0, (b) $\pi/4$, (c) $\pi/2$, and (d) $5\pi/6$, respectively.

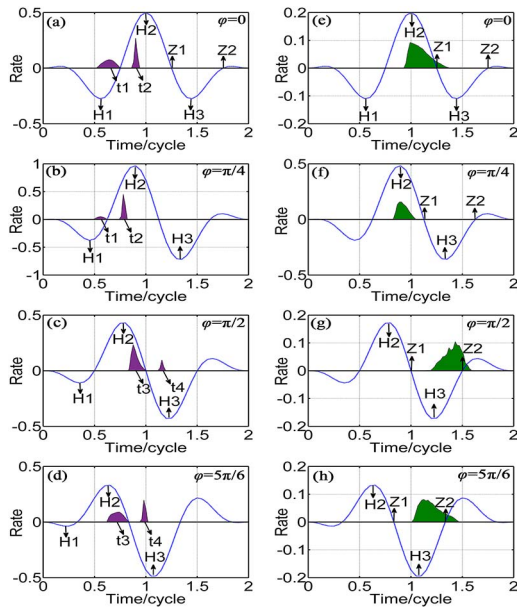


Fig. 4. (a) SI and (e) RC events [from Fig. 3(a)] versus time, (b) SI and (f) RC events [from Fig. 3(b)] versus time, (c) SI and (g) RC events [from Fig. 3(c)] versus time, (d) SI and (h) RC events from Fig. 3(d) versus time. The blue curves represent the laser field along the x direction.

in a previous study^[27]. Because the intensity of the peak H1 becomes lower with the increasing CEP, the first electron cannot pick up enough energy from the electric field. Specifically, the distribution of SI events undergoes a shift from the time t_1 (t_2) to the time t_3 (t_4) when CEP φ increases to $\pi/2$ [Fig. 4(c)]. As the CEP further increases to $5\pi/6$ [Fig. 4(d)], the number of SI events at time t_3 decreases, while the SI events at time t_4 increase. Figures 4(e)–4(h) show the corresponding RC events, where it is found that the RC time of the returning electron shifts to the adjacent half-cycle with the increasing CEP. According to SI time, there exist two types of corresponding RC events: RC events clustering around the zero crossing of the laser field and RC events near the peaks of the laser field.

To verify the above conclusion, we research the final momentum of electrons at different RC times in Fig. 5 and discover the shift of RC time corresponding to the appearance of the L-shaped structure. The RC time is divided into two parts according to the median. The corresponding CMD is also divided into two parts. Figures 5(a) and 5(b) show the CMDs for an RC time of the returning electron of less than $1.15T$ [close to the peak H2 in Fig. 4(e)] and greater than $1.15T$ (close to the zero crossing Z1) with the CEP of $\varphi = 0$, where the time $1.15T$ is median of RC time distribution in Fig. 4(e). In Fig. 5(a), two apparent regions locate above the anti-diagonal, indicating that most electrons are emitted outside the laser field in the back-to-back manner. This reflects anticorrelation behavior in Fig. 3(a). The momentum distribution in Fig. 5(b) is the primary composition of the first quadrant in Fig. 3(a). Figures 5(c) and 5(d) display CMDs for

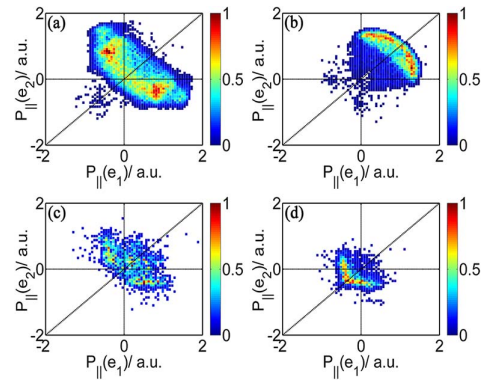


Fig. 5. CMDs of Ar atoms by linearly polarized two-cycle laser pulses at RC times (a) less than $1.15T$, (b) greater than $1.15T$ for the CEP of $\varphi = 0$, and (c) less than $1.4T$, (d) greater than $1.4T$ for the CEP of $\varphi = \pi/2$. The other parameters are the same as those in Fig. 3.

the RC time of returning electrons less than $1.4T$ [around the peak H3 in Fig. 4(g)] and greater than $1.4T$ (around the zero crossing Z2) with the CEP of $\varphi = \pi/2$, where the time $1.4T$ is the median of RC time distribution in Fig. 4(g). Obviously, the L-shaped structure in Fig. 3(c) is divided into two parts by the structures in Figs. 5(c) and 5(d). Two franks of the L-shaped region are made up of the back-to-back electrons in Fig. 5(c). The corner part of the L-shaped region is composed of the side-by-side electrons in Fig. 5(d). According to the above information, it is found that when RC events occur near the extremum of the laser field, two electrons tend to emit along the opposite directions, and one electron usually obtains smaller momentum along the negative direction, but another electron obtains larger momentum along the positive direction. However, when returning electrons collide with the parent core around the zero crossing of the laser field, in the end of the laser pulses, two electrons tend to emit into the same direction and both electrons may obtain larger momentum at the final state.

To explain the L-shaped structure, more details are obtained by inspecting the momentum and energy trajectories. Figure 6 depicts two typical energy trajectories [Figs. 6(a) and 6(b)] with a CEP of $\varphi = \pi/2$ and corresponding momentum trajectories [Figs. 6(c) and 6(d)]. According to the simple-man model^[28], when the returning electrons collide with the parent core near the peak of the laser field, these electrons usually obtain lower kinetic energy. However, when the returning electrons collide with the parent core around the zero crossing of the laser field, these electrons usually possess the larger kinetic energy. In Fig. 6(a), the red curve and blue curve denote returning electrons and bound electrons, respectively. When the red curve is first larger than zero, it indicates that the first electron is released via tunneling ionization. Subsequently, the red curve dramatically declines at time $1.3T$, which indicates that an RC event occurs at this moment, and the returning electron assigns only a part of the energy to the bound electron. This RC event occurs around

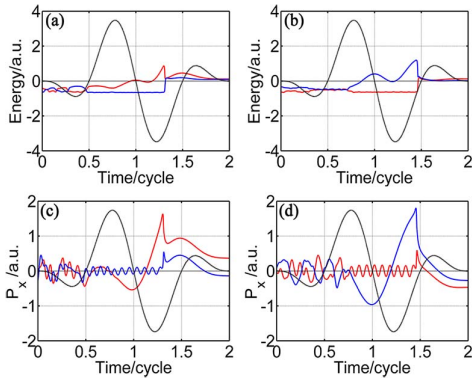


Fig. 6. (a) and (b) Two typical energy trajectories with CEP $\varphi = \pi/2$, and (c) and (d) corresponding momentum trajectories along the x direction. Black dashed lines denote the electric field of the laser pulses, blue and red curves denote the evolutions of the two electrons, and the other parameters are the same as those in Fig. 3(c).

the peak of the laser field. The energy of the returning electron before RC is 0.85 a.u. After RC, the returning electron still moves along the previous direction because of the remnant energy, as shown in Fig. 6(c). The bound electron will be ionized instantly after the RC. Subsequently, the movements of two electrons are dominated by the laser field. When the laser field changes its direction, the returning electron possesses higher energy than the second electron. These two electrons eventually emit into the opposite directions. Conversely, in Fig. 6(b), the blue curve denotes the returning electron. The RC event occurs around the zero crossing of the laser field. The energy of the returning electron before RC is 1.45 a.u. The returning electron shares a large proportion of energy to the bound electron right after RC, and its remnant energy is small. Then, the laser field quickly changes its direction, and both two electrons are primarily dominated by the subsequent laser field. The second electron quickly picks up energy from the electric field. Finally, the energy of the second electron is larger than that of the returning electron. The two electrons move toward the same direction, as shown in Fig. 6(d). According to statistical analysis of a large number of the above two kinds of momentum trajectories, it is found that the final momentum of one electron always changes from 0 a.u. to 0.5 a.u., but the momentum of the other electron slightly changes around 0.5 a.u., which reveals the formation of the L-shaped structure.

To further illustrate the above two types of RC trajectories accounting for the appearance of the L-shaped structure, we calculate the energy of the two electrons when RC events occur at times $1.3T$ [near the peak H3 in Fig. 4(g)] and $1.5T$ [near the zero crossing Z2 in Fig. 4(g)] and count the number of energy difference (ΔE), which implies the status of energy assignment between the two electrons right after RC. As shown in Figs. 7(a) and 7(b), the region A stands for effective RC events, and, in region B, one electron is bound. In

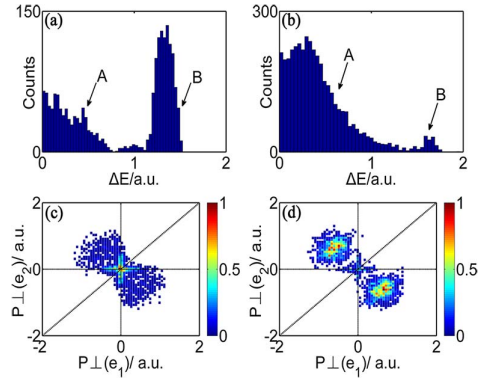


Fig. 7. Distributions of ΔE (the absolute value of the energy difference between the two electrons) at RC times (a) $1.3T$ and (b) $1.5T$ with CEP of $\varphi = \pi/2$, respectively. (c) and (d) are the corresponding transverse momentum spectra of the two electrons at two RC times. The other parameters are the same as those in Fig. 3.

Fig. 7(a), the returning electrons possess lower energy and assign a part of energy to ionize the second electron, so the ΔE is small, as shown in region A in Fig. 7(a). Sometimes, the energy of the returning electron is not enough to knock out the second electron, in this case, ΔE becomes larger, as shown in region B in Fig. 7(a). In Fig. 7(b), the RC electrons occurring around the zero crossing of the laser field share more energy to the bound electrons, where they may be recaptured by the ion core; in this case, ΔE is larger and changes from 0 to 1 a.u. Figures 7(c) and 7(d) depict the distributions of transverse momenta (perpendicular to the direction of laser field) at corresponding RC times. In Fig. 7(c), a large proportion of electrons distribute along the coordinate axes, which indicates different amplitudes of transverse momenta of the two electrons. In Fig. 7(d), the population is mainly located in the second and fourth quadrants, indicating the strong repulsion in the transverse direction. It is clear that if the energy of the RC electron is larger, the repulsion between the two electrons will be stronger, which provides evidence for the conclusion in Fig. 6. The asymmetric energy assignment plays an important role. This is similar to the conclusion of the study by Zhou *et al.*, where they analyze the asymmetric energy sharing from the distribution of transverse momentum^[29].

Using a classical ensemble method, we study NSDI of Ar atoms in ultrashort pulses with different CEPs. In four-cycle laser pulses, we verify the cross-like structure in the experiment. It is found that the CEP influences the shift of RC time and causes the transition of electrons in CMDs. The CEP effect is more obvious in two-cycle laser pulses. A special L-shaped structure appears in the CMD in two-cycle laser pulses when the CEP is $\varphi = \pi/2$. This structure reveals an unusual anticorrelated behavior. It is found that electrons recolliding with the parent core around the peak of the laser field will lead to the back-to-back electrons, while those RC events occurring near the zero crossing of the laser field will lead to

the side-by-side electrons. The CEP strongly influences the RC time of returning electrons, and the asymmetric energy assignment at different RC times plays an important role for the appearance of the L-shaped structure. Our study provides effective information for NSDI in few-cycle laser pulses.

This work was supported by the National Natural Science Foundation of China (No. 61275103) and the Natural Science Foundation of Shanghai (No. 18ZR1413600).

References

1. D. Liu, C. Chen, B. Man, Y. Sun, and F. Li, *Chin. Opt. Lett.* **14**, 040202 (2016).
2. M. Li, G. Zhang, T. Zhao, X. Ding, and J. Yao, *Chin. Opt. Lett.* **15**, 110201 (2017).
3. W. Becker, X. J. Liu, P. Ho, and J. H. Eberly, *Rev. Mod. Phys.* **84**, 1011 (2012).
4. C. F. de Morisson Faria and X. Liu, *J. Mod. Opt.* **58**, 1076 (2011).
5. D. Bauer, *Phys. Rev. A* **56**, 3028 (1997).
6. A. Rudenko, L. B. de Jesus, T. Ergler, K. Zrost, B. Feuerstein, C. D. Schröter, R. Moshhammer, and J. Ullrich, *Phys. Rev. Lett.* **99**, 263003 (2007).
7. S. Larochelle, A. Talebpour, and S. L. Chin, *J. Phys. B* **31**, 1201 (1998).
8. B. Yu and Y. Li, *Opt. Commun.* **304**, 87 (2013).
9. B. Yu, S. Jia, D. Zhang, and Q. Tang, *Opt. Commun.* **332**, 257 (2014).
10. B. Feuerstein, R. Moshhammer, D. Fischer, A. Dorn, C. D. Schröter, J. Deipenwisch, J. R. C. Lopez-Urrutia, C. Höhr, P. Neumayer, J. Ullrich, H. Rottke, C. Trump, M. Wittmann, G. Korn, and W. Sandner, *Phys. Rev. Lett.* **87**, 043003 (2001).
11. B. Schenkel, J. Biegert, U. Keller, C. Vozzi, M. Nisoli, G. Sansone, S. Stagira, S. De Silvestri, and O. Svelto, *Opt. Lett.* **28**, 1987 (2003).
12. J. Zhang, Z. Kong, Y. Liu, A. Wang, and Z. Zhang, *Photon. Res.* **4**, 27 (2016).
13. W. Tang, J. Zhao, K. Yang, S. Zhao, G. Li, D. Li, T. Li, and W. Qiao, *Photon. Res.* **5**, 46 (2017).
14. X. Liu, *Phys. Rev. Lett.* **92**, 133006 (2004).
15. Y. Zhou, Q. Liao, Q. Zhang, W. Hong, and P. Lu, *Opt. Express* **18**, 632 (2010).
16. K. O'Keeffe, P. Jöchl, H. Drexel, V. Grill, F. Krausz, and M. Lezius, *Appl. Phys. B* **78**, 583 (2004).
17. Q. Liao, P. Lu, Q. Zhang, W. Hong, and Z. Yang, *J. Phys. B* **41**, 125601 (2008).
18. N. G. Johnson, O. Herrwerth, A. Wirth, S. De, I. Ben-Itzhak, M. Lezius, F. Krausz, B. Bergues, M. F. Kling, A. Sentleben, C. D. Schröter, R. Moshhammer, J. Ullrich, K. J. Betsch, R. R. Jones, A. M. Saylor, T. Rathje, K. Rühle, W. Müller, and G. G. Paulus, *Phys. Rev. A* **83**, 013412 (2011).
19. B. Bergues, M. Kuel, N. G. Johnson, B. Fischer, N. Camus, K. J. Betsch, O. Herrwerth, A. Sentleben, A. M. Saylor, T. Rathje, I. Ben-Itzhak, R. R. Jones, G. G. Paulus, F. Krausz, R. Moshhammer, J. Ullrich, and M. F. Kling, *Nat. Commun.* **3**, 813 (2012).
20. D. Ye, X. Liu, and J. Liu, *Phys. Rev. Lett.* **101**, 233003 (2008).
21. C. Huang, Y. Zhou, Q. Zhang, and P. Lu, *Opt. Express* **21**, 11382 (2013).
22. Z. Zhang, J. Zhang, L. Bai, and X. Wang, *Opt. Express* **23**, 7044 (2015).
23. Y. Zhou, C. Huang, A. Tong, Q. Liao, and P. Lu, *Opt. Express* **19**, 2301 (2011).
24. R. Panfili, J. H. Eberly, and S. L. Haan, *Opt. Express* **8**, 431 (2001).
25. R. Panfili, S. L. Haan, and J. H. Eberly, *Phys. Rev. Lett.* **89**, 113001 (2002).
26. Z. Zhang, L. Bai, and J. Zhang, *Phys. Rev. A* **90**, 023410 (2014).
27. Y. Zhou, Q. Liao, P. Lan, and P. Lu, *Chin. Phys. Lett.* **25**, 3950 (2008).
28. P. B. Corkum, *Phys. Rev. Lett.* **71**, 1994 (1993).
29. Y. Zhou, Q. Liao, and P. Lu, *Phys. Rev. A* **82**, 053402 (2010).